Dalton Transactions

ROYAL SOCIETY OF CHEMISTRY

PAPER

View Article Online
View Journal | View Issue

Cite this: *Dalton Trans.*, 2021, **50**, 8558

Nonanuclear zinc–gold [Zn_3Au_6] heterobimetallic complexes†

Ravi Yadav, Milena Dahlen, Akhil K. Singh, Xiaofei Sun, Michael T. Gamer and Peter W. Roesky *

Received 27th April 2021,
Accepted 19th May 2021

DOI: 10.1039/d1dt01396c

rsc.li/dalton

Nonanuclear zinc–gold heterobimetallic complexes were synthesized in a two-step process. Commercially available carboxy-functionalized phosphine ligands were used for selective binding to Zn and Au centers. In the first step, bipyridine coordinated Zn-metalloligands with free phosphine moieties were prepared. Reaction of Zn-metalloligands with [AuCl(tht)] (tht = tetrahydrothiophene) resulted in the formation of nonanuclear Zn–Au heterobimetallic complexes. The flexibility of the carboxy-functionalized phosphine ligands was shown to be crucial for the formation of aurophilic interactions. Further, the photoluminescence of the Zn-metalloligands and one Zn–Au complex was investigated at room temperature as well as 77 K. The emission spectra showed clear difference between the Zn-metalloligands and the Zn–Au complex.

Introduction

The investigation of heterobimetallic complexes is one of the forefront topics in modern inorganic chemistry.[1,2] Growing interest in this area could be attributed to the applications of heterobimetallic complexes as efficient catalysts in various organic transformations.[2–4] Besides, the utility of heterometallic complexes is not limited to catalysis as they have shown potential application as luminescent materials,[5–10] in medicinal as well as materials science.[11,12] Within the rising demand for tailor made catalysts and materials featuring specific sets of properties, heterometallic complexes pose a promising approach. The properties in heterobimetallic systems can be fine-tuned by choosing different sets of metal or by modifying the ligand motifs between the metal centres.[13–16] In this context, development of methodologies for the design of new combinations of different metals is an active research area.[15,17–20] The use of bifunctional ligands, for example based on the Pearson's hard soft acid–base (HSAB) concept, is an interesting approach.[9,21] Orthogonal binding site are hereby crucial for a selective synthesis.[22,23] A successfully established combination is *e.g.* the incorporation of phosphine (soft donor) and carboxylate (hard donor) moieties within the same ligand framework.[11,18,24–27]

The reported heterobimetallic complexes based on HSAB concept are dominated by early–late heterobimetallic complexes.[3,28,29] Since it is established that Zn[30–34] and Au[35–38] form luminescent complexes each, we anticipated that a combination of both metals might be beneficial. Recently, we reported d^{10}–d^{10} (Zn–Au) heterobimetallic complexes using bipyridine functionalized carbene ligands and investigated their photophysical properties.[21] However, the ligand synthesis in this system is sophisticated. Therefore, we felt challenged to synthesize larger Zn/Au complexes by using easily accessible ligand systems. Carboxy-functionalized phosphine ligands are commercially available. They have been used before to synthesize Ru–Zn or Sn–Au heterobimetallic complexes.[26,27] However, to the best of our knowledge, such ligand system has not been reported yet incorporating the particular combination of Zn(II) and Au(I). Herein, we present nonanuclear [Zn_3Au_6] heterobimetallic complexes featuring a trinuclear zinc-carboxylate central core and peripheral phosphine bound [AuCl] moieties. The bifunctional carboxyl-phosphine ligands were chosen to selectively bind to zinc and gold centers. By altering the ligands rigidity, aurophilic interactions could be induced.

Results and discussion

Zinc based metalloligands

The synthesis of Zn–Au heterobimetallic complexes was performed in a two-step process. First, zinc complexes were synthesized, which were subsequently used as metalloligands for complexation of gold chloride. Latter approach is a convenient

Institute of Inorganic Chemistry, Karlsruhe Institute of Technology (KIT), Engesserstraße 15, 76131 Karlsruhe, Germany. E-mail: roesky@kit.edu

† Electronic supplementary information (ESI) available. CCDC 2051757–2051760. For ESI and crystallographic data in CIF or other electronic format see DOI: 10.1039/d1dt01396c

and selective route towards heterometallic complexes, which has been used amongst others also by our group.[9,11,39]

We synthesized two different metalloligands (**1** and **2**, Fig. 1) with different spacer lengths between the respective functional groups. Due to the resulting different flexibility, we anticipated the formation of different heterobimetallic complexes. It has been shown previously that the degree of aurophilic interactions in bimetallic M–Au complexes depends on the flexibility of the ligand used.[24,25]

For the synthesis of the first zinc-based metalloligand, $[(Bipy)Zn(Me)_2]$[40] (Bipy = 2,2′-bipyridine) was treated with 4-(diphenylphosphino)benzoic acid (**H–L^{Ph}**) in a 1 : 2 molar ratio (Scheme 1). The complex $[(Bipy)Zn(p\text{-}O_2C\text{-}C_6H_4\text{-}PPh_2)_2]$ (**1**) was isolated as colorless crystals in 70% yield. The ^{1}H NMR spectrum exclusively shows resonances in the aromatic region, (δ = 7.28–9.14 ppm), corresponding to the aryl groups of the phosphine and bipyridine moiety. The $^{31}P\{^1H\}$ NMR spectrum shows a singlet resonance at δ = −5.2 ppm, a typical chemical shift for non-coordinated triarylphosphines.[24] The identity of **1** was further established by single crystal X-ray diffraction studies. Complex **1** crystallized in the triclinic space group $P\bar{1}$ with one molecule in the asymmetric unit (Fig. 2). The solid state structure revealed the Zn atom being coordinated by a chelating bipyridine and three oxygen atoms of two carboxylate ligands. The Zn–N1 (2.0667(12) Å) and Zn–N2 (2.0868(12) Å) bond distances are in the typical range for bipyridine zinc-carboxylate moieties (2.057(7)–2.100(8) Å).[41–43] Interestingly, the two **L^{Ph}** ligands around the Zn center exhibit different coordination modes *i.e.* mono- (κ^1) and bidentate (κ^2) mode. Owing to the monodentate coordination, the Zn–O1 (1.9207(10) Å) bond length is slightly shorter than that of Zn–O3 (1.9809(10) Å).[44,45] However, the Zn–O4 bond length is significantly longer (2.4785(11) Å), suggesting a weak interaction as compared to the Zn–O3 and Zn–O1 bonds. The two **L^{Ph}** ligands are widely tilted apart from each other with a P1–Zn–P2 angle of 146.30(9)°.

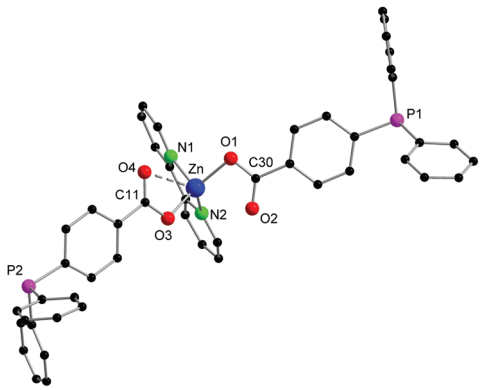

Fig. 2 Molecular structure of complex **1** in the solid state. Hydrogen atoms are omitted for clarity. Selected bond lengths (Å) and angles [°]: Zn–N1 2.0667(12), Zn–N2 2.0868(12), Zn–O1 1.9207(10), Zn–O3 1.9809(10), Zn–O4 2.4785(11), O1–C11 1.2873(2), O2–C11 1.231(2), O3–C30 1.275(2), O4–C30 1.240(2); O1–Zn–O3 127.40(5), O1–Zn–O4 101.73(4), O3–Zn–O4 57.73(4), O3–Zn–O4 57.73(4), O2–C11–O1 123.72(13), O4–C30–O3 121.73(13).

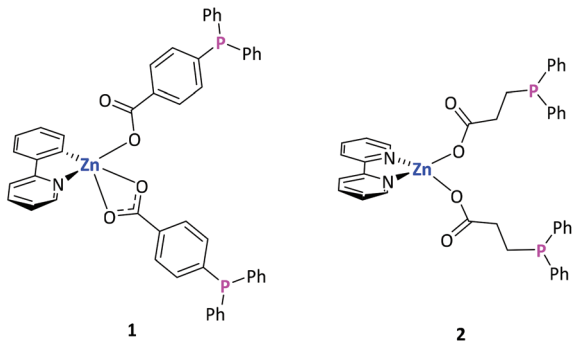

Fig. 1 Metalloligands **1** and **2**.

In the IR spectrum of **1**, we observed strong bands for the asymmetric COO^- stretching mode. One double peak is seen at 1615 and 1606 cm^{-1}, which we assign to the κ^1-coordinated benzoate, while another peak is seen at 1550 cm^{-1}, which may be assigned to the κ^2-bound benzoate group.[46]

To obtain the second metalloligand, we employed 3-(diphenylphosphino)propionic acid (**H–L^{Et}**) promising a more flexible ligand scaffold due to the ethylene spacer between its functional groups. Reaction of $[(Bipy)Zn(Me)_2]$ with **H–L^{Et}** in a 1 : 2 molar ratio resulted $[(Bipy)Zn(O_2C\text{-}C_2H_4\text{-}PPh_2)_2]$ (**2**) in 62% yield (Scheme 2). The ^{1}H NMR spectrum of **2** shows a set of multiplet resonances in the range of δ = 2.32–2.43 ppm, corresponding to the ethyl unit of the **L^{Et}** ligand. Multiplet resonances in the aromatic region (δ = 7.25–8.98 ppm) can be assigned to the aryl protons of the phosphine and bipyridine ligands. The $^{31}P\{^1H\}$ NMR spectrum shows a single resonance

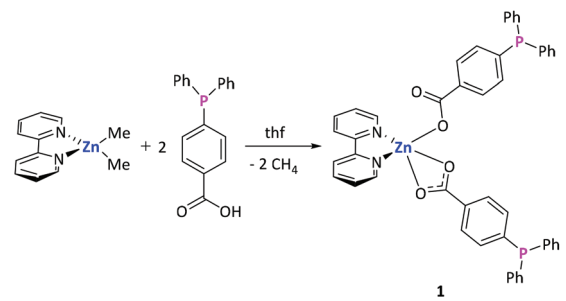

Scheme 1 Synthesis of complex **1**.

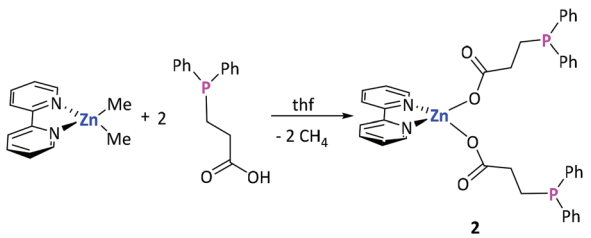

Scheme 2 Synthesis of complex **2**.

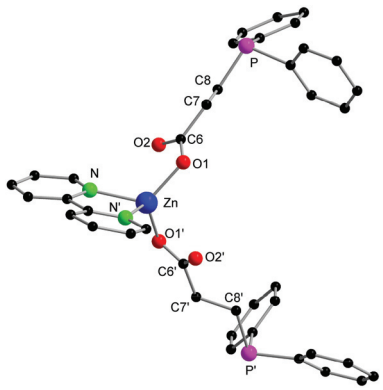

Fig. 3 Molecular structure of complex **2** in the solid state. Hydrogen atoms are omitted for clarity. Selected bond lengths (Å) and angles [°]: Zn–N 2.056(3), Zn–O1 1.939(2), O1–C6 1.286(4), O2–C6 1.235(4); O1–Zn–O1′ 118.3(2), N–Zn–N′ 79.7(2), O2–C6–O1 122.5(3).

at δ = −14.7 ppm being in accordance with uncoordinated diphenyl phosphine moieties.[25]

Complex **2** crystallizes in the orthorhombic space group *Aea*2 with half a molecule in the asymmetric unit cell (Fig. 3). The Zn atom is tetra coordinated by a chelating bipyridine unit and by each one oxygen atom of the two carboxylate ligands. In contrast to **1**, both carboxylates are κ^1-coordinated. The Zn–N bond length (2.056(3) Å) in complex **2** is insignificantly shorter than that in complex **1** (2.0667(12) Å and 2.0868(12) Å). The Zn–O bond lengths (1.939(2) Å) in complex **2** are also similar to the respective κ^1-coordinated carboxylate group (Zn1–O1 1.9207(10) Å) in complex **1**.

Zn–Au nonanuclear heterobimetallic complexes

Bimetallic complexes were obtained by reacting the metalloligands **1** and **2** with [AuCl(tht)][47] (tht = tetrahydrothiophene) (Schemes 3 and 4). The reaction between **1** and [AuCl(tht)] in thf at room temperature resulted in coordination of the phosphine moieties to [AuCl] (Scheme 3 and Fig. 4). Successful coordination was confirmed by $^{31}P\{^1H\}$ NMR, showing a broad resonance at δ = 33.5 ppm, which is downfield shifted by 38.7 ppm compared to complex **1**.[24] In the ^1H NMR spectrum of the product, the resonances for the aromatic protons are also slightly downfield shifted upon coordination of the phosphine donors to [AuCl].[24] The reaction mixture was dissolved in a mixture of solvents (a 1 : 1 : 1

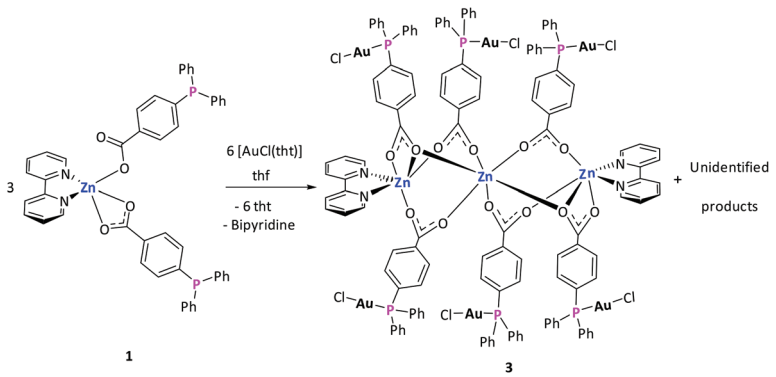

Scheme 3 Synthesis of complex **3**.

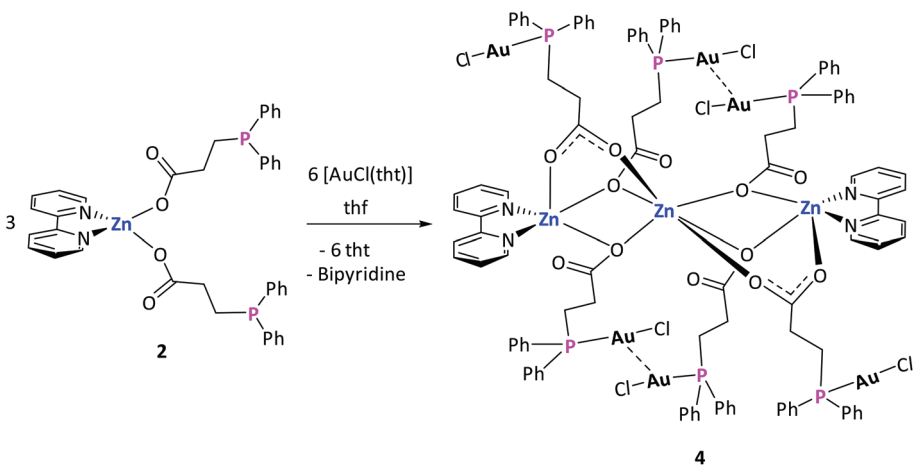

Scheme 4 Synthesis of complex **4**.

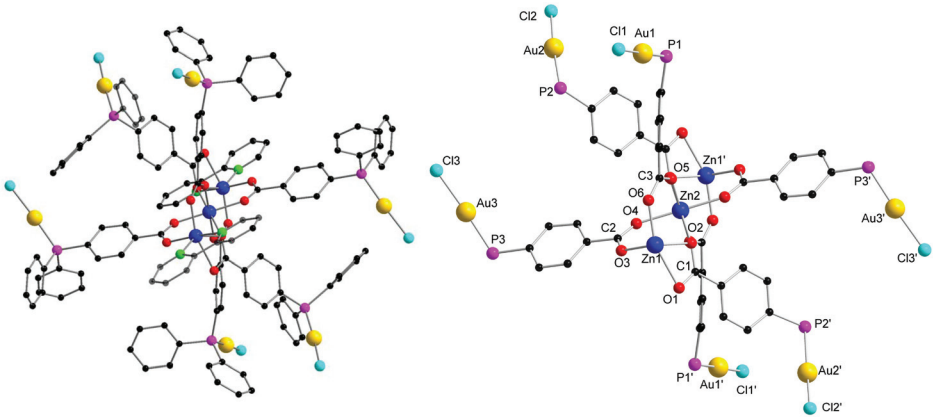

Fig. 4 Left: Molecular structure of complex **3** in the solid state. Right: Molecular structure of complex **3** with omitted, bipyridines and phenyl groups for clarity. Hydrogen atoms and solvent molecules are omitted for clarity. Selected bond lengths (Å) and angles [°]: Au1–Cl1 2.283(2), Au2–Cl2 2.270(2), Au3–Cl3 2.296(3), Au1–P1 2.220(2), Au2–P2 2.160(2), Au3–P3 2.224(2), Zn1–O1 2.279(6), Zn1–O2 2.137(5), Zn1–O3 2.022(5), Zn1–O6 2.029(5), Zn1–N1 2.114(6), Zn1–N2 2.159(6), Zn1–C1 2.535(7), Zn2–O2 2.182(5), Zn2–O2 2.182(5) Zn2–O4 2.068(5), Zn2–O4 2.068(5), Zn2–O5 2.053(5), Zn2–O5 2.053(5), O1–C1 1.228(9), O2–C1 1.290(9), O3–C2 1.255(9), O4–C2 1.253(8), O5–C3 1.250(9), O6–C3 1.263(9); P1–Au1–Cl1 178.97(8), P2–Au2–Cl2 169.9(8), P3–Au3–Cl3 177.34(9), O1–C1–O2 121.2(7), O4–C2–O3 127.5(7), O5–C3–O6 126.3(6).

solution of dichloromethane, acetone and ethanol) and allowed to crystallize by slow evaporation. A few colorless crystals were obtained along with white amorphous solid. X-ray diffraction analysis of the colorless crystals revealed the formation of the nonanuclear complex $[(Bipy)_2Zn_3\{(p\text{-}O_2C\text{-}C_6H_4\text{-}PPh_2)AuCl\}_6]$ (**3**) (Fig. 4). During the reaction, one Bipy ligand got lost from the central Zn atom. The resulting vacant coordination sites were filled by bridging carboxylate groups from the other zinc atoms. Complex **3** crystallizes in the triclinic space group $P\bar{1}$ with half a molecule of **3**, half a molecule of ethanol, and one molecule of acetone in the asymmetric unit. Each zinc atom is hexa coordinated, both Zn1 and Zn1′ are coordinated by the nitrogen atoms of chelating bipyridine ligands and fourfold coordinated by the oxygen atoms of the carboxylate part of $\mathbf{L^{Ph}}$ ligands. In contrast, Zn2 is only coordinated by O atoms of the carboxylate parts of all the six $\mathbf{L^{Ph}}$ ligands.

The carboxylate moieties in complex **3** show two different coordination modes, κ^2 and κ^3. The Zn–N bond distances in complex **3** are elongated in comparison to those in complex **1** (2.136 *vs.* 2.077 Å, respectively). This elongation can be attributed to a higher coordination number of the Zn atoms in **3** and a stronger coordination from the carboxylate group of $\mathbf{L^{Ph}}$ (Zn1–O 2.022–2.279 Å). The Zn2–O bond distances are in the range from 2.053 Å to 2.182 Å. The average P–Au bond length (2.201 Å) is as expected for triarylphosphines coordinated to AuCl moieties.[48,49] The Au–Cl bond lengths (from 2.270 to 2.296 Å) are in agreement with the previously reported values for phosphine-coordinated AuCl complexes.[48,49] Interestingly, the three Zn atoms and the bipyridine ligands are coplanar. Surprisingly, no intra- or inter-molecular aurophilic interaction (expected Au–Au distances 2.70–3.50 Å)[35,48,50–52] was observed in the nonanuclear assembly of **3**. This may be the result of steric crowding and rigidity of the triarylphosphine ligand. Despite several attempts, complex **3** could not be obtained in analytically pure form due to the formation of an unidentified white precipitate (*vide supra*).

For comparison, the coordination chemistry of the more flexible zinc-based metalloligand **2** towards gold(I) was studied next. Reaction of **2** with [AuCl(tht)] resulted nonanuclear complex $[(Bipy)_2Zn_3\{(O_2C\text{-}C_2H_4\text{-}PPh_2)AuCl\}_6]$ (**4**) (Scheme 4), isolated in 68% yield. Single crystal X-ray diffraction analysis confirmed the formation of **4** (Fig. 5). Complex **4** crystallizes in the triclinic space group $P\bar{1}$ with half of a molecule of **4** and two molecules of THF in the asymmetric unit cell. Similar to the synthesis of **3**, a nonanuclear Zn_3Au_6 complex is formed *via* loss of one bipyridine molecule. The three Zn atoms in complex **4** are arranged in similar manner as in complex **2**. The terminal Zn1 and Zn1′ atoms are coordinated by bipyridine ligands and $\mathbf{L^{Et}}$ carboxylate moieties while central Zn2 is only surrounded by carboxylate ligands.

The Zn1 and Zn1′ atoms are penta-coordinated, exhibiting a square pyramidal coordination geometry, while Zn2 is in an octahedral coordination environment. In complex **4**, the Zn1–N1 (2.137(3) Å) and Zn1–N2 (2.108(4) Å) bond distances are elongated as compared to the Zn–N bond length in complex **3** (2.056(3) Å). The oxygen atoms of the carboxylate groups are arranged in two different coordination modes, κ^1 and κ^2, and the Zn–O bond lengths (from 1.994(3) to 2.177(3) Å) are in the expected range. The Au–P bond lengths (2.2308(9)–2.2404(10) Å) are also in the expected area of phosphine coordination to a [AuCl] moiety. Interestingly, Au–Au interactions are observed between four out of the six Au atoms. The Au1–Au2 distance (3.3512(3) Å) is within the range of aurophilic interactions and could be classified as semi-supported contacts.[35,48,50–52] As observed in complex **2**, the bipyridine nitrogen atoms and the three Zn atoms in complex **4** are in one plane and the gold-coordinated phosphine ligands are attached *via* the carboxylate group. Unlike **3**, complex **4** could be successfully isolated in an analytically pure form. In the

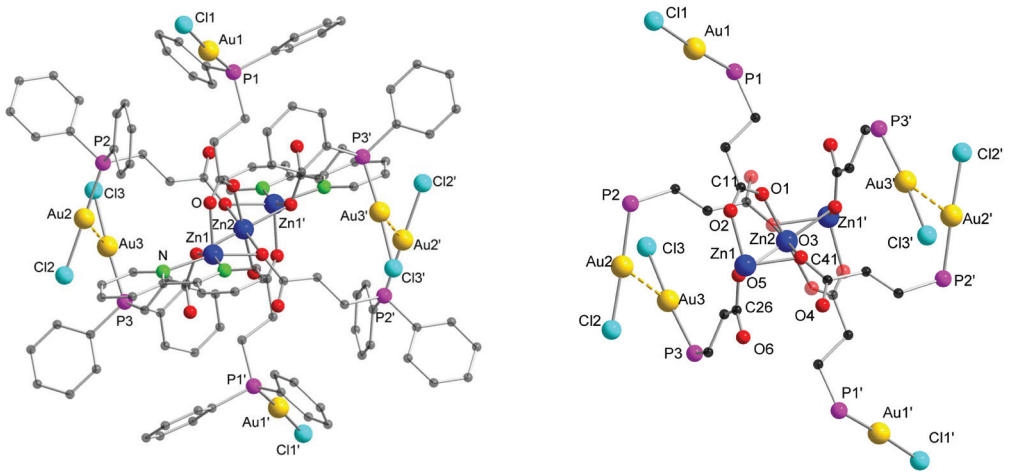

Fig. 5 Left: Molecular structure of complex **4** in the solid state. Right: Molecular structure of complex **4** with omitted, bipyridines and phenyl groups for clarity. Hydrogen atoms and solvent molecules are omitted for clarity. Selected bond lengths (Å) and angles [°]: Au2–Au3 3.3512(3), Au1–Cl1 2.2810(11), Au2–Cl2 2.2845(11), Au3–Cl3 2.2903(12), Au1–P1 2.2308(9), Au2–P2 2.2346(9), Au3–P3 2.2404(10), Zn1–O1 2.003(3), Zn1–O3 2.177(3), Zn1–O5 2.150(2), Zn2–O2 1.994(3), Zn2–O3 2.056(3), Zn2–O5 2.053(3), Zn2–N1 2.137(3), Zn2–N2 2.108(4), O1–C11 1.268(4), O2–C11 1.249(4), O3–C41 1.298(5), O4–C41 1.206(5), O5–C26 1.300(5), O6–C26 1.222(5); P1–Au1–Cl1 175.61(4), P2–Au2–Cl2 172.80(5), P3–Au3–Cl3 175.05(5), O2–C11–O1 126.1(3), O6–C26–O5 124.1(3), O4–C41–O3 123.3(4).

case of **4**, the selective aggregation by aurophilic interactions is presumably facilitated by the flexibility of the $\mathbf{L^{Et}}$ ligand.

In contrast to one multiplet at δ = 2.32–2.43 ppm observed in complex **2**, the ^{1}H NMR spectrum of **4** shows two multiplets at δ = 2.54–2.60 ppm and 2.73–2.79 ppm, corresponding to the protons of the $\mathbf{L^{Et}}$ ethyl group. The relative integration ratio of 1 : 3 between the protons of bipyridine and $\mathbf{L^{Et}}$ ligands, respectively, supports the formation of nonanuclear complex **4**. Coordination of the phosphine donors to [AuCl] moieties in complex **4** is supported by a single resonance at δ = 29.6 ppm in the ^{31}P{^{1}H} NMR spectrum, which is significantly downfield shifted compared to **2** (δ = −14.7 ppm).[25]

We have carried out low temperature NMR studies to observe some intermediate for the formation of complex **4**. An NMR reaction between complex **2** and 2 equivalents of [AuCl(tht)] in $CDCl_3$ was started at −55 °C (Fig. S17†). At −55 °C, the ^{31}P{^{1}H} NMR spectrum showed a signal δ = 29 ppm for complex **4** and a broad resonance at δ = 40 ppm (possible intermediate). Upon increasing the temperature, the broad resonance at δ = 40 ppm disappears at 15 °C. The variable temperature NMR study showed that complex **4** is formed through some intermediate but the exact nature of the intermediate remains elusive.

Photoluminescence properties

The presented Zn and Zn–Au complexes appear white to yellow in the solid state. When irradiated with a UV lamp (λ_{Exc} = 365 nm), **1** and **4** show yellow and bluish luminescence, respectively, whilst **2** is barely luminescent at room temperature (see Fig. 6). We have investigated the photophysical properties at 298 K and 77 K.

Except for a red-shift of about 30 nm for **2**, emission spectra at 77 K for **1** and **2** look very similar. Both zinc compounds feature a broad unstructured emission band with maxima at λ_{Max} = 544 nm (**1**) and λ_{Max} = 580 nm (**2**). The excitation onset is at ~375 nm (**1**) and ~400 nm for **2** (both 77 K) and features a narrower band for latter compared to **1**. For both structures, luminescence intensity decreases upon warming up to room temperature. However, despite their structural similarity, luminescence of compound **1** is still visible at room temperature while that of **2** is too weak to be detected. This difference could be tentatively assigned to the smaller conjugated system present in **2**. For **1** and **2**, emission decay times were found to be in the nanosecond range (up to ~280 ns, see ESI† for more details), indicating fluorescence emission. While in terms of shape, observed spectra resemble those in literature for similar complexes also displaying a broad emission with no visible vibronic pattern, λ_{Max} of **1** and **2** is significantly more redshifted.[53] Emission properties are probably attributed to ligand based transitions as also indicated by theoretical calculations (see below). Complexation of the zinc ion enhances the ligands conformational rigidity, reducing the non-radiative relaxation of the ligand based excited states.[54]

Interestingly, compound **4** displays a well resolved vibronic pattern at low temperatures (77 K), which is still visible at room temperature indicating a different relaxation mechanism. The excitation onset is blue-shifted to ~350 nm compared to **1** and **2** and the emission band shows three maxima at 77 K: λ_{Max} = 444 nm, 474 nm and 502 nm. Also, an additional small shoulder at ~540 nm was observed. At low temperatures, three different lifetimes were observed: one is in the same timescale as for **1** and **2** (~5 ns), possibly belonging to the ligand-based transitions. A possible second lifetime was detected in the single-digit microsecond range but could be

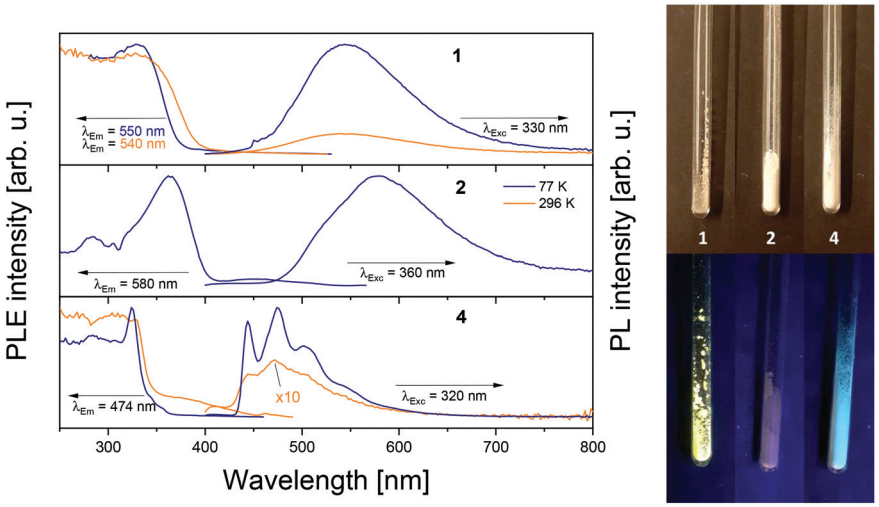

Fig. 6 Left: Solid state photoluminescence emission (PL) and excitation (PLE) spectra of **1**, **2** and **4** (polycrystalline samples) at different temperatures with the depicted emission and excitation wavelengths. PL of **2** is not displayed at 295 K due to a very low signal. Right: Photographs of compounds **1**, **2** and **4** at daylight (top) and under UV light (λ_{Exc} = 365 nm) (bottom).

determined thoroughly (see ESI† for details). The third shows a long phosphorescence decay with ~2 ms which might be attributed to the heavy metal effect caused by the gold atoms present in **4**. Latter effect is know from literature, saying that an intersystem crossing (ISC) mechanism is facilitated due to an enhanced spin–orbit coupling.[55] Metallophilic interactions might also contribute as they are known to contribute to photoluminescence properties.[55] Emission intensity of all aforementioned compounds strongly decreases by increasing the temperature, mirrored also in the shortening of the PL lifetimes.

Quantum chemical calculations

To gain more insight into the photophysical properties, time-dependent density functional theory calculations were performed for complexes **1**, **2** and **4** using the Gaussian 16 package (for details see the ESI†). Calculations reproduced the experimentally observed absorption and emission properties. We were not able to carry out excited state geometries for complex **4** due to its larger size. However, we have successfully calculated singlet, triplet ground state geometries and absorption properties. The calculated absorption and emission properties of complexes are listed in Table S4.† The MO analysis (Fig. S22–S25†) reveals that S1, S2 and S3 states of complex **1** and **2**, are either intra-ligand charge transfer (ILCT) or ligand to ligand charge transfer (LLCT). For these excited states, the donating orbital represents phosphine and bipyridine moieties in complex **1**, while only phosphine moieties in complex **2**. The accepting LUMOs are localized on both, the phosphine and the bipyridine backbone. Similarly, in the singlet ground state donor and acceptor orbitals in complex **4** are mainly localized on the ligand while triplet states are more interesting. In the triplet state donating orbitals are associated with d_{Z_2} orbitals of gold atoms (HOMO−49, HOMO−50) and accepting orbital are mainly found on bipyridine moieties suggesting metal to metal to ligand charge transfer (MMLCT) as previously reported metallophilic interaction induced luminescent complexes.[55]

Conclusions

With the aim to provide easily accessible metalloligands, zinc-metalloligands supported by commercially available bifunctional phosphine-carboxylate ligands featuring different spacers between the two donor groups have been synthesized. As donor groups we chose phosphine units, which are able to coordinate soft metal atoms. As example, we showcase the coordination of gold(I) ions. However, the extension of this chemistry to a larger number of other metal combinations seems possible.

Upon coordination of the phosphine donors of the metalloligands to [AuCl] moieties, unprecedented nonanuclear heterobimetallic complexes were formed by the loss of one bipyridine ligand. The lability of the bipyridine ligand, which was at the first glance surprising, seems to be the key point for the formation of polynuclear complexes. While no aurophilic interaction was observed in the complex featuring the $\mathbf{L}^{\mathbf{Ph}}$ ligand, the $\mathbf{L}^{\mathbf{Et}}$-supported complex featured short Au···Au separations and intramolecular aurophilic interactions. Such a difference in the molecular arrangements may be ascribed to the distinct flexibility of the ligands and hence different steric crowding around the Au metal centers. Analytics were completed by photophysical investigation of complexes **1**, **2** and **4**. Whilst **2** shows only weak photoluminescence, **1** and **4** express high luminescence at lower temperature which is still visible at room temperature. Additionally, **2** and **4** show a distinct difference in the shape of the emission band, well displaying the coordination of the gold atoms. The experimental findings were further corroborated by theoretical studies. Theoretical

calculations showed ILCT and LLCT in monometallic complexes **1** and **2**. In bimetallic complex **4**, calculations suggested MMLCT.

Experimental

General procedures

All manipulations of air- and water-sensitive reactions were performed with rigorous exclusion of oxygen and moisture in flame-dried Schlenk-type glassware either on a dual manifold Schlenk line, interfaced to a high vacuum (10^{-3} torr) line or in an argon-filled MBraun glove box. Solvents were dried using an MBraun solvent purification system (SPS 800) and subsequently degassed and stored *in vacuo* over $LiAlH_4$. Elemental analyses were carried out with an Elementar vario Micro cube. $CDCl_3$ was distilled over P_2O_5 and stored over 3 Å molecular sieves. IR spectra were obtained on a Bruker Tensor 37 spectrometer equipped with a room temperature DLaTGS detector and a diamond ATR (attenuated total reflection) unit. ^1H, $^{13}C\{^1H\}$, and $^{31}P\{^1H\}$ NMR spectra were recorded on a Bruker Avance Neo or Avance III 400 (^1H: 400.30 MHz, ^{13}C: 100.67 MHz, ^{31}P: 162.04 MHz) or on a Bruker Avance 300 (^1H: 300.13 MHz, ^{13}C: 75.48 MHz, ^{31}P: 121.50 MHz). The chemical shifts are reported in ppm relative to external TMS (^1H, ^{13}C) and H_3PO_4 (85%) (^{31}P). The multiplicity of the signals is indicated as s = singlet, d = doublet, t = triplet, sept = septet, m = multiplet and br = broad. [(Bipy)Zn(Me)$_2$][40] and [AuCl(tht)][47] were synthesized according to the reported procedure. 4-(Diphenylphosphino)benzoic acid (97%) (**H–L^{Ph}**) and 3-(diphenylphosphino)propionic acid (97%) (**H–L^{Et}**) were purchased from Acros Organics and used as received.

Synthesis of [(Bipy)Zn(*p*-O$_2$CPhPPh$_2$)$_2$] (1).[56] Pre-cooled (*ca.* −30 °C) thf (15 mL) was added to a Schlenk flask containing a mixture of [(Bipy)Zn(Me)$_2$] (126 mg, 0.500 mmol) and **H–L^{Ph}** (306 mg, 1.00 mmol) *via* cannula. The color of the reaction mixture quickly changed from light yellow to colorless indicating the formation of complex **1**. The solution was allowed to warm to room temperature, stirred for 6 h, and all the volatiles were removed under reduced pressure. The resulting solid was recrystallized by slow evaporation of a solution of **1** in dichloromethane and toluene (2 : 1). The crystals were washed with 5 mL of ice-cold diethylether and 2 × 5 mL of pentane and dried *in vacuo*. **Yield** = 70% (292 mg, 0.35 mmol). **Anal. calcd** for $C_{48}H_{36}N_2O_4P_2Zn$ (832.15): C, 69.28; H, 4.36; N, 3.37. **Found**: C, 69.93; H, 4.09; N, 3.67. **^{1}H NMR** (400 MHz, 298 K, $CDCl_3$): δ [ppm] = 7.27–7.34 (m, 24 H, Ph-*H*), 7.62 (br, 2 H, NCHC*H*, $\Delta\nu_{1/2} \approx 16$ Hz), 8.02–8.06 (m, 6 H, NCHCHC*H* & Ph-*H*), 8.20 (br, 2 H, NCC*H*, $\Delta\nu_{1/2} \approx 14$ Hz), 9.13 (br, 2 H, NC*H*CH, $\Delta\nu_{1/2} \approx 18$ Hz). **^{31}P{^{1}H} NMR** (162 MHz, 298 K, $CDCl_3$): δ [ppm] = −5.2 (s, *P*Ph$_2$Ar). **^{13}C{^{1}H} NMR** (100 MHz, 298 K, $CDCl_3$): δ [ppm] = 121.2 (NC*C*H), 126.7 (NCH*C*H), 128.7 (d, *m*-C_{Ph}, $^3J_{CP}$ = 7.0 Hz), 129.0 (*p*-C_{Ph}), 130.2 (d, *m*-C_{PhCOO}, $^3J_{CP}$ = 7.0 Hz), 132.8 (i-C_{PhCOO}), 133.1 (d, *o*-C_{PhCOO}, $^2J_{CP}$ = 19.5 Hz), 134.0 (d, *o*-C_{Ph}, $^2J_{CP}$ = 20 Hz), 136.8 (d, i-*C*P, $^1J_{CP}$ = 10.6 Hz), 140.5 (NCHCH*C*H), 142.1 (d, i*C*P, $^1J_{CP}$ = 12.5 Hz), 150.3 (N*C*HCH), 174.5 (*C*OOR), no signal could be detected for the N*C*CH of bipyridine ligand. **IR (ATR)**: ν (cm^{-1}) = 3056 (vw), 1615 (s), 1606 (s, ν_{COO}), 1594 (m, ν_{COO}), 1550 (m, ν_{COO}), 1535 (w), 1490 (m), 1473 (m), 1445 (s), 1435 (s), 1391 (s), 1391 (s), 1376 (s), 1361 (m), 1299 (w), 1250 (w), 1234 (m), 1200 (m), 1176 (w), 1155 (m), 1135 (w), 1088 (m), 1070 (m), 1058 (m), 1028 (m), 1015 (m), 999 (m), 983 (w), 912 (w), 855 (s), 846 (s), 812 (w), 779 (vs), 768 (vs), 752 (vs), 737 (vs), 723 (vs), 704 (vs), 692 (m), 650 (m), 633 (w), 586 (w), 554 (w), 542 (m), 526 (s), 504 (w), 481 (m), 433 (m), 413 (s).

Synthesis of [(Bipy)Zn(O$_2$C-C$_2$H$_4$-PPh$_2$)$_2$] (2).[56] To a mixture of [(Bipy)Zn(Me)$_2$] (126 mg, 0.500 mmol) and **H–L^{Et}** (258 mg, 1.00 mmol) pre-cooled (*ca.* −30 °C) thf (15 mL) was added. As observed in the synthesis of **1**, the reaction mixture quickly turned from light yellow to colorless. The reaction mixture was allowed to warm to room temperature and subsequently stirred for 6 hours. Crystals of **2** suitable for X-ray diffraction studies were grown by slow vapor diffusion of pentane in a thf solution of the complex. The mother liquor was separated by decantation and the crystals were dried under vacuum. **Yield** = 62% (250 mg, 0.340 mmol). **Anal. calcd** for $C_{40}H_{36}N_2O_4P_2Zn$ (736.07): C, 65.27; H, 4.93; N, 3.81. **Found**: C, 65.49; H, 4.73; N, 3.69. **^{1}H NMR** (400 MHz, 298 K, $CDCl_3$): δ [ppm] = 2.32–2.43 (m, 8 H, C*H*$_2$C*H*$_2$), 7.25–7.27 (m, 12 H, Ph-*H*), 7.36–7.40 (m, 8 H, Ph-*H*), 7.60 (br, 2 H, NCHC*H*, $\Delta\nu_{1/2} \approx 20$ Hz), 8.05 (t, 2 H, NCHCHC*H*, $^3J_{HH}$ = 7.0 Hz), 8.17 (d, 2 H, NCC*H*, $^3J_{HH}$ = 8.0 Hz), 8.98 (br, 2 H, NC*H*CH, $\Delta\nu_{1/2} \approx 13$ Hz). **^{31}P{^{1}H} NMR** (162 MHz, 298 K, $CDCl_3$): δ [ppm] = −14.7 (s, 2 P, CH_2PPh_2). **^{13}C{^{1}H} NMR** (100 MHz, 298 K, $CDCl_3$): δ [ppm] = 24.3 (d, *C*H$_2$PPh$_2$, $^1J_{CP}$ = 11 Hz), 31.6 (d, *C*H$_2$CO$_2$, $^2J_{CP}$ = 18 Hz), 121.0 (NC*C*H), 126.8 (NCH*C*H), 128.4 (d, *m*-C_{Ph}, $^3J_{CP}$ = 6.5 Hz), 128.5 (*p*-C_{Ph}), 133.9 (d, *o*-C_{Ph}, $^2J_{CP}$ = 18 Hz), 138.6 (d, i-*C*P, $^1J_{CP}$ = 12 Hz), 140.6 (NCHCH*C*H), 150.3 (N*C*HCH), 180.6 (d, *C*O$_2$R, $^3J_{CP}$ = 16 Hz), no signal could be detected for N*C*CH. **IR (ATR)**: ν (cm^{-1}) = 3071 (vw), 3019 (vw), 2952 (vw), 2908 (vw), 1708 (w), 1612 (s, ν_{COO}), 1600 (s, ν_{COO}), 1569 (w), 1476 (m), 1450 (m), 1434 (m), 1399 (s), 1319 (m), 1292 (s), 1270 (m), 1255 (m), 1195 (w), 1161 (m), 1099 (m), 1067 (w), 1043 (w), 1026 (m), 999 (w), 949 (w), 935 (w), 851 (vw), 826 (vw), 785 (vs), 753 (s), 742 (vs), 699 (vs), 681 (w), 659 (w), 637 (w), 610 (w), 527 (m), 513 (s), 475 (s), 432 (s).

Synthesis of [(Bipy)$_2$Zn$_3${(*p*-O$_2$CPhPPh$_2$)AuCl}$_6$] (3).[56] To a mixture of **1** (100 mg, 0.120 mmol) and [AuCl(tht)] (77.0 mg, 0.24 mmol) was added thf (10 mL). The reaction mixture was stirred at room temperature for 3 hours. All the volatiles were removed *in vacuo*. The product was washed with 2 × 5 mL of pentane and dried under vacuum. A few crystals of **3** suitable for X-ray diffraction studies were obtained along with some white amorphous solid by evaporation of a solution of the crude product in dichloromethane, acetone, and ethanol in 1 : 1 : 1 ratio. Despite several attempts analytically pure complex **3** could not be prepared in a bulk quantity. Analytical data of crude product from the reaction between **1** and [AuCl(tht)]. **^{1}H NMR** (400 MHz, 298 K, $CDCl_3$): δ [ppm] = 7.43–7.51 (m, 24 H, Ph-*H*), 7.69 (t, 2 H, NCHC*H*, $^3J_{HH}$ = 6.0 Hz), 8.06 (t, 2 H, NCHCHC*H*, $^3J_{HH}$ = 6.0 Hz), 8.19 (d, 4 H, Ph-*H*, $^3J_{HH}$ = 8.1

Hz), 8.27 (d, 2 H, NCC*H*, $^{3}J_{HH}$ = 8.0 Hz), 9.14 (d, 2 H, NC*H*CH, $^{3}J_{HH}$ = 4.5 Hz). The ratio of integration of protons of the crude products does not fit with the formulation of **3**. **^{31}P{^{1}H} NMR** (162 MHz, 298 K, $CDCl_3$): δ [ppm] = 33.4 (br, *P*-AuCl, $\Delta\nu_{1/2} \approx$ 120 Hz). **^{13}C{^{1}H} NMR** (100 MHz, 298 K, $CDCl_3$): δ [ppm] = 121.4 (NC*C*H), 127.0 (NCH*C*H), 128.6 (d, i-*C*P, $^{1}J_{CP}$ = 30 Hz), 129.4 (d, C_{Ph}, $^{1}J_{CP}$ = 6.0 Hz), 129.4 (d, C_{Ph}, J_{CP} = 12 Hz), 131.0 (d, C_{Ph}, J_{CP} = 12 Hz), 132.2 (C_{Ph}), 133.7 (d, C_{Ph}, J_{CP} = 14 Hz), 134.2 (d, C_{Ph}, J_{CP} = 14 Hz), 137.3 (C_{Ph}), 141.0 (NCHCH*C*H), 149.3 (N*C*CH), 150.3 (N*C*HCH), no signal could be detected for *C*OOR. **IR (ATR):** ν (cm^{-1}) = 3056 (vw), 2945 (vw), 2883 (vw), 2839 (vw), 1599 (m, ν_{COO}), 1586 (m), 1538 (m), 1538 (m), 1493 (w), 1475 (m), 1436 (s), 1415 (s), 1389 (s), 1315 (w), 1306 (w), 1253 (w), 1186 (w), 1158 (w), 1101 (s), 1058 (w), 1027 (m), 1016 (m), 998 (m), 974 (w), 861 (w), 779 (s), 766 (s), 748 (vs), 732 (s), 713 (s), 700 (vs), 691 (vs), 654 (w), 633 (w), 618 (vw), 565 (m), 533 (s), 504 (s), 483 (w), 456 (s).

Synthesis of $[(Bipy)_2Zn_3\{(O_2C\text{-}C_2H_4\text{-}PPh_2)AuCl\}_6]$ (4).[56] To a mixture of **2** (100 mg, 0.135 mmol) and [AuCl(tht)] (87 mg, 0.217 mmol) was added thf (10 mL). The reaction mixture was stirred for 3 hours at room temperature. All the volatiles were removed *in vacuo*. The residue was washed with 2 × 5 mL of pentane and dried under vacuum to obtain complex **4** as a white solid. The product was dissolved in minimum amount of thf and allowed to stand in the dark at room temperature. After few weeks crystals of **4** suitable for X-ray diffraction studies were obtained. **Yield** = 68% (104 mg, 0.015 mmol). **Anal. calcd** for $C_{110}H_{100}N_4O_{12}P_6Cl_6Au_6Zn_3$ (3442.51): C, 38.33; H, 2.92; N, 1.63. **Found**: C, 38.45; H, 3.18; N, 1.60. **^{1}H NMR** (400 MHz, 298 K, $CDCl_3$): δ [ppm] = 2.54–2.60 (m, 12 H, PCH_2), 2.73–2.79 (m, 12 H, CH_2CO_2), 7.41–7.54 (m, 36 H, Ph-*H*), 7.61–7.67 (m, 24 H, Ph-*H*), 7.69 (t, 4 H, NCHC*H*, $^{3}J_{HH}$ = 6.3 Hz), 8.14 (t, 4 H, NCHCHC*H*, $^{3}J_{HH}$ = 6.7 Hz), 8.23 (d, 4 H, NCC*H*, $^{3}J_{HH}$ = 8.0 Hz), 8.95 (d, 4 H, NC*H*CH, $^{3}J_{HH}$ = 4.8 Hz). **^{31}P{^{1}H} NMR** (162 MHz, 298 K, $CDCl_3$): δ [ppm] = 29.5 (s, *P*-AuCl). **^{13}C{^{1}H} NMR** (100 MHz, 298 K, $CDCl_3$): δ [ppm] = 24.4 (d, *C*H_2PPh_2, $^{1}J_{CP}$ = 39.7 Hz), 30.6 (*C*H_2CO_2), 121.2 (NC*C*H), 127.2 (NCH*C*H), 129.3 (*p*-C_{Ph}), 129.4 (d, *m*-C_{Ph}, $^{3}J_{CP}$ = 11.5 Hz), 132.2 (d, *o*-C_{Ph}, $^{2}J_{CP}$ = 2.9 Hz), 133.4 (d, i-*C*P, $^{1}J_{CP}$ = 13 Hz), 141.1 (NCHCH*C*H), 149.0 (N*C*CH), 150.2 (N*C*HCH), 177.4 (d, *C*O_2R, $^{3}J_{CP}$ = 18 Hz). **IR (ATR):** ν (cm^{-1}) = 3058 (vw), 3025 (vw), 2925 (vw), 2850 (vw), 1703 (w), 1598 (m, ν_{COO}), 1493 (w), 1474 (m), 1435 (m), 1376 (vw), 1314 (vw), 1265 (vw), 1184 (vw), 1157 (vw), 1104 (m), 1026 (vw), 998 (vw), 954 (vw), 901 (vw), 795 (vs), 769 (s), 738 (s), 693 (vs), 652 (w), 632 (w), 521 (s), 486 (s), 466 (w), 434 (w), 416 (w).

Conflicts of interest

There are no conflicts to declare.

Acknowledgements

RY and PWR acknowledge funding for the current project from the SFB 1176 funded by the German Research Foundation (DFG). M.D. thanks the "Fonds der Chemischen Industrie" for the generous fellowship (Nr. 103581). We thank Prof. Dr D. Fenske for measuring the single crystal (**4**) and Karlsruhe Nano Micro Facility (KNMF) for measuring time.

Notes and references

1 J. A. Mata, F. E. Hahn and E. Peris, *Chem. Sci.*, 2014, **5**, 1723–1732.
2 P. Buchwalter, J. Rosé and P. Braunstein, *Chem. Rev.*, 2015, **115**, 28–126.
3 B. G. Cooper, J. W. Napoline and C. M. Thomas, *Catal. Rev.*, 2012, **54**, 1–40.
4 K. M. Gramigna, D. A. Dickie, B. M. Foxman and C. M. Thomas, *ACS Catal.*, 2019, **9**, 3153–3164.
5 Q.-M. Wang, Y.-A. Lee, O. Crespo, J. Deaton, C. Tang, H. J. Gysling, M. C. Gimeno, C. Larraz, M. D. Villacampa, A. Laguna and R. Eisenberg, *J. Am. Chem. Soc.*, 2004, **126**, 9488–9489.
6 U. Helmstedt, S. Lebedkin, T. Höcher, S. Blaurock and E. Hey-Hawkins, *Inorg. Chem.*, 2008, **47**, 5815–5820.
7 R. Feng, L. Chen, Q.-H. Chen, X.-C. Shan, Y.-L. Gai, F.-L. Jiang and M.-C. Hong, *Cryst. Growth Des.*, 2011, **11**, 1705–1712.
8 J. R. Shakirova, E. V. Grachova, V. V. Gurzhiy, I. O. Koshevoy, A. S. Melnikov, O. V. Sizova, S. P. Tunik and A. Laguna, *Dalton Trans.*, 2012, **41**, 2941–2949.
9 S. Bestgen, C. Schoo, C. Zovko, R. Köppe, R. P. Kelly, S. Lebedkin, M. M. Kappes and P. W. Roesky, *Chem. – Eur. J.*, 2016, **22**, 7115–7126.
10 N. D. Knöfel, H. Rothfuss, P. Tzvetkova, B. Kulendran, C. Barner-Kowollik and P. W. Roesky, *Chem. Sci.*, 2020, **11**, 10331–10336.
11 J. Fernández-Gallardo, B. T. Elie, F. J. Sulzmaier, M. Sanaú, J. W. Ramos and M. Contel, *Organometallics*, 2014, **33**, 6669–6681.
12 H. Han, Z. Zhou, J. C. Carozza, J. Lengyel, Y. Yao, Z. Wei and E. V. Dikarev, *Chem. Commun.*, 2019, **55**, 7243–7246.
13 L. H. Gade, *Angew. Chem., Int. Ed.*, 2000, **39**, 2658–2678.
14 P. Braunstein, X. Morise, M. Bénard, M.-M. Rohmer and R. Welter, *Chem. Commun.*, 2003, 610–611.
15 C. Fliedel, A. Ghisolfi and P. Braunstein, *Chem. Rev.*, 2016, **116**, 9237–9304.
16 R. Yadav, T. Simler, M. T. Gamer, R. Köppe and P. W. Roesky, *Chem. Commun.*, 2019, **55**, 5765–5768.
17 K. Mashima, H. Nakano and A. Nakamura, *J. Am. Chem. Soc.*, 1996, **118**, 9083–9095.
18 P. Braunstein, *Chem. Rev.*, 2006, **106**, 134–159.
19 J. Goura and V. Chandrasekhar, *Chem. Rev.*, 2015, **115**, 6854–6965.
20 R. Yadav, M. E. Hossain, R. Peedika Paramban, T. Simler, C. Schoo, J. Wang, G. B. Deacon, P. C. Junk and P. W. Roesky, *Dalton Trans.*, 2020, **49**, 7701–7707.

21 C. Kaub, S. Lebedkin, A. Li, S. V. Kruppa, P. H. Strebert, M. M. Kappes, C. Riehn and P. W. Roesky, *Chem. – Eur. J.*, 2018, **24**, 6094–6104.
22 F. Völcker, F. M. Mück, K. D. Vogiatzis, K. Fink and P. W. Roesky, *Chem. Commun.*, 2015, **51**, 11761–11764.
23 F. Völcker and P. W. Roesky, *Dalton Trans.*, 2016, **45**, 9429–9435.
24 N. D. Knöfel, C. Schweigert, T. J. Feuerstein, C. Schoo, N. Reinfandt, A.-N. Unterreiner and P. W. Roesky, *Inorg. Chem.*, 2018, **57**, 9364–9375.
25 N. D. Knöfel, C. Schoo, T. P. Seifert and P. W. Roesky, *Dalton Trans.*, 2020, **49**, 1513–1521.
26 G. Amenuvor, J. Darkwa and B. C. E. Makhubela, *Catal. Sci. Technol.*, 2018, **8**, 2370–2380.
27 C. Jobbágy, P. Baranyai, Á. Gömöry and A. Deák, *CrystEngComm*, 2018, **20**, 5935–5939.
28 R. M. Bullock and C. P. Casey, *Acc. Chem. Res.*, 1987, **20**, 167–173.
29 N. Wheatley and P. Kalck, *Chem. Rev.*, 1999, **99**, 3379–3420.
30 Y. Ma, H.-Y. Chao, Y. Wu, S. T. Lee, W.-Y. Yu and C.-M. Che, *Chem. Commun.*, 1998, 2491–2492.
31 S. Wang, *Coord. Chem. Rev.*, 2001, **215**, 79–98.
32 G. A. Ardizzoia, S. Brenna, S. Durini, B. Therrien and M. Veronelli, *Eur. J. Inorg. Chem.*, 2014, **2014**, 4310–4319.
33 S. Bestgen, C. Schoo, B. L. Neumeier, T. J. Feuerstein, C. Zovko, R. Köppe, C. Feldmann and P. W. Roesky, *Angew. Chem., Int. Ed.*, 2018, **57**, 14265–14269.
34 J. Xiong, K. Li, T. Teng, X. Chang, Y. Wei, C. Wu and C. Yang, *Chem. – Eur. J.*, 2020, **26**, 6887–6893.
35 H. Schmidbaur and A. Schier, *Chem. Soc. Rev.*, 2008, **37**, 1931–1951.
36 V. W.-W. Yam and E. C.-C. Cheng, *Chem. Soc. Rev.*, 2008, **37**, 1806–1813.
37 R. Visbal, I. Ospino, J. M. López-de-Luzuriaga, A. Laguna and M. C. Gimeno, *J. Am. Chem. Soc.*, 2013, **135**, 4712–4715.
38 T. P. Seifert, V. R. Naina, T. J. Feuerstein, N. D. Knöfel and P. W. Roesky, *Nanoscale*, 2020, **12**, 20065–20088.
39 F. Zhang, X.-M. Cao, J. Wang, J. Jiao, Y. Huang, M. Shi, P. Braunstein and J. Zhang, *Chem. Commun.*, 2018, **54**, 5736–5739.
40 K.-H. Thiele and H. Rau, *Z. Anorg. Allg. Chem.*, 1967, **353**, 127–134.
41 M. Amin Hasan, N. Kumari, P. Kumar, B. Pathak and L. Mishra, *Polyhedron*, 2013, **50**, 306–313.
42 B. Murugesapandian and P. W. Roesky, *Inorg. Chem.*, 2011, **50**, 1698–1704.
43 M. T. Ng, T. C. Deivaraj, W. T. Klooster, G. J. McIntyre and J. J. Vittal, *Chem. – Eur. J.*, 2004, **10**, 5853–5859.
44 J. He, Y. Wang, W. Bi, X. Zhu and R. Cao, *J. Mol. Struct.*, 2006, **787**, 63–68.
45 Y.-F. Zhou, R.-H. Wang, B.-L. Wu, R. Cao and M.-C. Hong, *J. Mol. Struct.*, 2004, **697**, 73–79.
46 C. C. R. Sutton, G. da Silva and G. V. Franks, *Chem. – Eur. J.*, 2015, **21**, 6801–6805.
47 S. Ahrland, K. Dreisch, B. Norén and Å. Oskarsson, *Mater. Chem. Phys.*, 1993, **35**, 281–289.
48 A. S. K. Hashmi, I. Braun, M. Rudolph and F. Rominger, *Organometallics*, 2012, **31**, 644–661.
49 C. Sarcher, A. Lühl, F. C. Falk, S. Lebedkin, M. Kühn, C. Wang, J. Paradies, M. M. Kappes, W. Klopper and P. W. Roesky, *Eur. J. Inorg. Chem.*, 2012, 5033–5042.
50 P. Pyykkö, *Angew. Chem., Int. Ed.*, 2004, **43**, 4412–4456.
51 A. S. K. Hashmi, M. Wieteck, I. Braun, P. Nösel, L. Jongbloed, M. Rudolph and F. Rominger, *Adv. Synth. Catal.*, 2012, **354**, 555–562.
52 H. Schmidbaur and A. Schier, *Chem. Soc. Rev.*, 2012, **41**, 370–412.
53 G. H. Eom, H. M. Park, M. Y. Hyun, S. P. Jang, C. Kim, J. H. Lee, S. J. Lee, S.-J. Kim and Y. Kim, *Polyhedron*, 2011, **30**, 1555–1564.
54 S.-M. Yue, H.-B. Xu, J.-F. Ma, Z.-M. Su, Y.-H. Kan and H.-J. Zhang, *Polyhedron*, 2006, **25**, 635–644.
55 V. W.-W. Yam and E. Chung-Chin Cheng, in *Photochemistry and photophysics of coordination compounds II*, eds. V. Balzani, S. Campagna and A. Barbieri, Springer, Berlin, Heidelberg, 2007, vol. 281, pp. 269–309.
56 R. Yadav, *Synthesis of Heterometallic Zinc-Gold and Lanthanide-Transition Metal carbonyl complexes and Reactivity Study of Pentaphosphaferrocene Towards Low-Valent Main Group Species*, PhD Thesis, Karlsruhe Institute of Technology (KIT), Kalrsruhe, Germany, 2019.